Hg^+ Frequency Standards

John D. Prestage, Robert L. Tjoelker and Lute Maleki

California Institute of Technology, Jet Propulsion Laboratory
4800 Oak Grove Drive
Building 298
Pasadena, CA 91104

Abstract. In this paper we review the development of Hg^+ microwave frequency standards for use in high reliability and continuous operation applications. In recent work we have demonstrated short-term frequency stability of $3\times10^{-14}/\sqrt{\tau}$ when a cryogenic oscillator of stability $2\text{-}3\times10^{-15}$ was used as the local oscillator. The trapped ion frequency standard employs a ^{202}Hg discharge lamp to optically pump the trapped $^{199}Hg^+$ clock ions and a helium buffer gas to cool the ions to near room temperature. We describe a small Hg^+ ion trap based frequency standard with an extended linear ion trap (LITE) architecture which separates the optical state selection region from the clock resonance region. This separation allows the use of novel trap configurations in the resonance region since no optical pumping is carried out there. A method for measuring the size of an ion cloud inside a linear trap with a 12-rod trap is currently being investigated. At $\sim10^{-12}$, the 2nd order Doppler shift for trapped mercury ion frequency standards is one of the largest frequency offsets and its measurement to the 1-% level would represent an advance in insuring the very long-term stability of these standards to the 10^{-14} or better level. Finally, we describe atomic clock comparison experiments that can probe for a time variation of the fine structure constant, $\alpha = e^2/2\pi hc$, at the level of 10^{-20}/year as predicted in some Grand Unified String Theories.

INTRODUCTION

A small, continuously operating atomic clock with stability of 10^{-15} or better would advance the art and science of spacecraft navigation in deep space and enable space-based tests of general relativity that far exceed the sensitivities of earth-based tests. Similarly, continuously operating earth-based clocks with stability approaching 10^{-16} for averaging intervals between 1000 and 10,000 seconds would enhance the search for low frequency gravitational waves via careful Doppler tracking of the Cassini spacecraft en route to Saturn. These goals have defined and shaped the technologies used for the development of the ultra-stable linear ion trap Hg^+ at the JPL Frequency Standards Lab. Because ions in a trap undergo very weak hyperfine population relaxation rates, ^{202}Hg rf discharge lamps can substantially optically pump $^{199}Hg^+$ ions into the F=0 ground hyperfine level in a second or so. Pumping into this state proceeds with the scattering of only a few uv photons per ion and thus, a high signal-to-noise ratio in the measured clock resonance can only be achieved with large ion clouds, typically with 10^6 to 10^7 ions. Motivated by these constraints, we first recognized and developed the linear ion trap [1] for storage of ion clouds that were ten or more times larger than could be stored in a conventional Paul trap. Because the linear trap replaces the point node of the Paul trap with a line of nodes, there is no increase in Doppler shift from the excess rf micro-motion caused by space charge repulsion of ions from the vicinity of the node region.

We have built 10 frequency standards based on Hg ions in a linear trap, seven of the style shown in Figure 1 (LITS) [2] and three of the extended type (LITE) [3] as shown in Figure 4. Both the LITS and the LITE architectures have demonstrated frequency stability well into the 10^{-16}-stability range.

RECENT RESULTS WITH LITS/CSO COMBINATION

Figure 1 shows the configuration for the original Linear Ion Trap Standard (LITS). Ions are loaded into the trap with an electron pulse injected along the trap axis that ionizes a vapor of isotopically enriched ^{199}Hg atoms at a pressure of 10^{-9} Torr or less. This low pressure vapor is generated by heating a mercuric oxide (HgO) powder to 200C or higher.

With a background base vacuum system pressure of a few $x10^{-10}$ Torr, ion-trapping times of a few hours can be achieved.

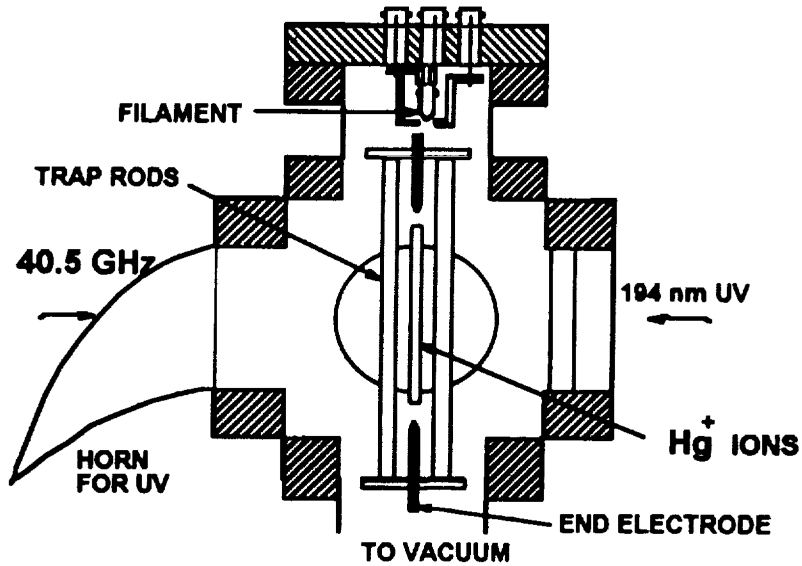

FIGURE 1. The linear ion trap based frequency standard is shown above. The trap is housed in a titanium vacuum cube. The molybdenum trap rods are 5 mm in diameter and are mounted on a 20.3 mm circle. The endcap electrodes are separated by 75 mm. State selection light from a ^{202}Hg discharge lamp enters from the right, is focused onto the central 1/3 of the trapped ions, and is collected in the horn. Fluorescence from the ions is collected in both directions normal to the page.

The LITS has shown excellent signal-to-noise in the measured clock transition and is determined by the size of the ion resonance line and the level of stray light output from the ^{202}Hg lamp. Signal levels as high as 80,000 with a background stray light rate of about 180,000 have been measured in a 1.5-second collection interval with dual fluorescence collection optical modules. These signal levels were measured with an 8 second Ramsey interrogation of the 40.5 GHz Hg^{+} clock transition and will yield a clock performance $\sigma_y(\tau) = 2x10^{-14}/\sqrt{\tau}$ as calculated from signal-to-noise and line Q. This short term performance exceeds the noise level for all but the very best short term stable oscillators, even the best H-masers available in our lab.

Recently, a cryogenic compensated sapphire oscillator (CSO) [4] has been developed in our lab and has been used to measure the un-degraded LITS performance. This continuously operating cryo-cooled liquid Helium refrigerated sapphire cavity oscillator delivers short-term stability of a few $x10^{-15}$ to a few hundred seconds and is adequate to measure the ion standard short term performance. The LITS standard is compared to the Compensated Sapphire Oscillator [4] as shown in the schematic configuration of Figure 2. During this measurement the LITS calculated stability from signal-to-noise and line-Q was approximately $3x10^{-14}/\sqrt{\tau}$ as was measured. This shows that for short-term performance there are no additional noise sources larger than shot noise of the total collected uv light.

Another measurement shown schematically in Figure 2 is steering the CSO to follow the ion clock resonance and compare that output to a SAO hydrogen maser. This shows that the LITS-CSO combination at $3x10^{-14}/\sqrt{\tau}$, exceeds the hydrogen maser stability for all averaging time intervals over the duration of this measurement. This measurement was carried out with a large ion cloud with a second order Doppler shift of over 10^{-12} and consequently, a potential for noise sources from Doppler instabilities. For this reason and in order to reduce the size of the LITS we have changed the architecture of the LITS clock to exploit the mobility of charged ions and that they can be electrically transported from one end of a linear trap to another.

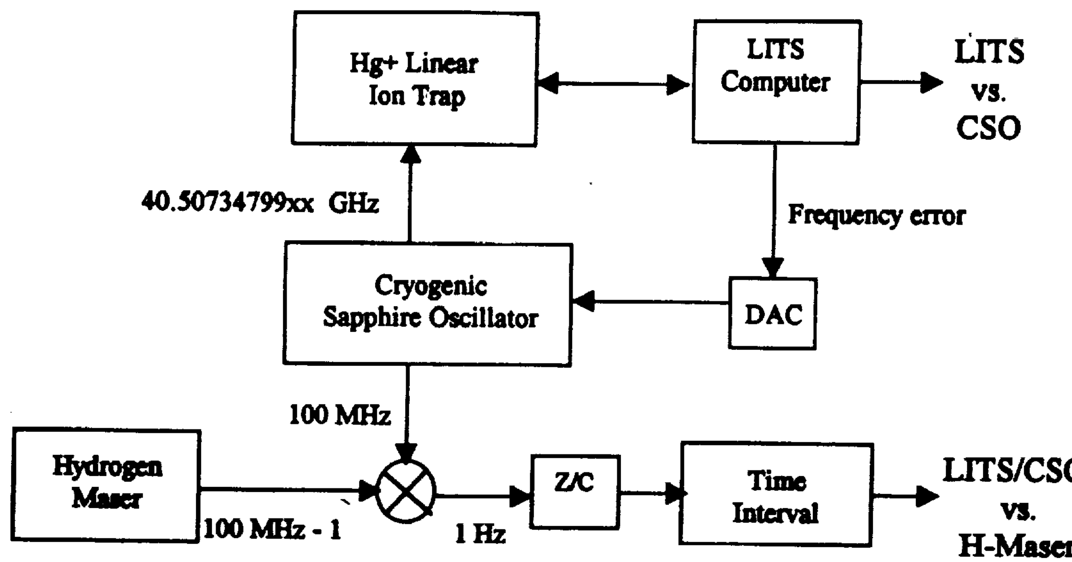

Figure 2. Schematic of the method used to measure the LITS short-term frequency stability against the ultra-stable cryo-cooled sapphire oscillator. Also shown here is the measurement of the frequency stability of the LITS/CSO combination compared to the stability of a hydrogen maser.

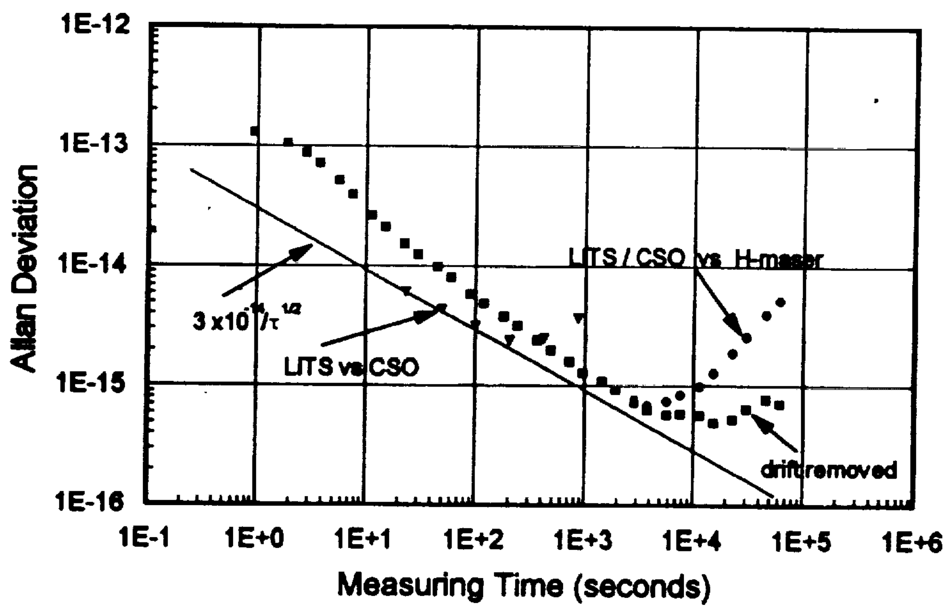

Figure 3. The measured Allan Deviation of the LITS vs CSO (inverted triangles) and the LITS steering the CSO vs a hydrogen maser (circles). The LITS vs CSO data demonstrates that for times less than 200 seconds, where the CSO is better than the LITS, the LITS stability is $3\times10^{-14}/\sqrt{\tau}$, better than any passive atomic frequency standard has demonstrated. In the second measurement shown here, the LITS steers the CSO to remove its degrading stability beyond 200 seconds. The LITS/CSO combination exceeds H-maser stability for the duration of the measurement interval.

LINEAR ION TRAP EXTENDED (LITE)

One modification to the LITS architecture that we are investigating is the extended linear ion trap shown in Figure 4. This layout partitions a linear trap into an optical interrogation region, similar to that shown in Figure 1, and adds an extension to carry out the microwave clock transition. The ions are moved from one region to another via a ~5 volt dc voltage bias applied to the trapping rods of that region. There are several advantages to the LITE architecture over the LITS arrangement where the magnetic shields surround the full optical system. In the LITE, the lamp and its rf exciter are outside the magnetic shields which will isolate it both electrically and thermally from the ion resonance region. The lamp exciter dissipates 10-20 Watts at ~170 MHz and can cause temperature variations of the vacuum chamber and stray, unshielded magnetic fields in the ion resonance region. Similarly, ground return currents in the bias feeds to the resistively heated filament, and filament emission grid collection leads, photo-multiplier high voltage supplies, etc. are all inside the multi-layer magnetic shielding of the LITS, unlike in the LITE shown below. In addition, the optical trap region and the resonance trap regions can be designed separately to address each of the two distinct functions. The resonance trap can be designed to allow the ion cloud second order Doppler shift to be measured and that design is described in the next section.

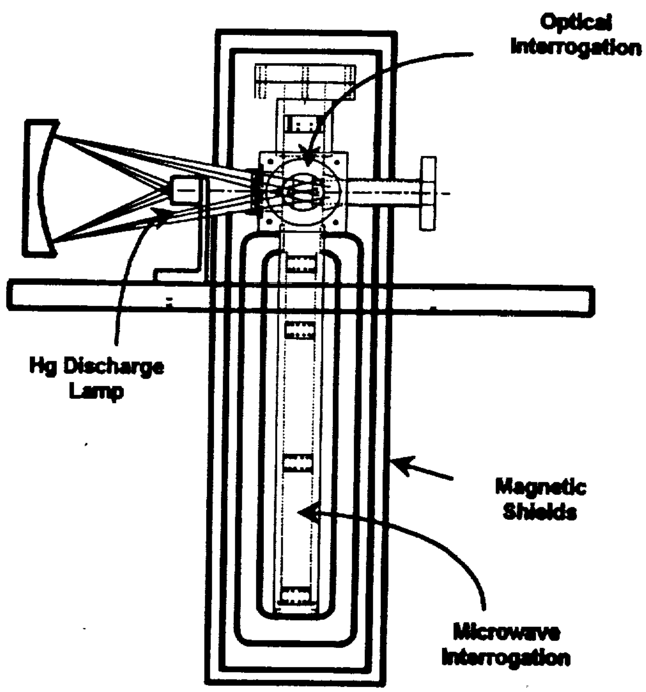

Figure 4. The Linear Ion Trap extended (LITE). The two distinct tasks of optical state selection/preparation and microwave interrogation are carried out in separate regions. Ions are electrically transported from one region to the other by a dc bias on the rods to exclude ions from either region.

HARMONIC LINEAR ION TRAPS

The harmonicity of a traditional four-rod linear ion trap is a function of rod diameter and spacing. Improved harmonicity can be accomplished with variations to this geometry. For example, figure 5 shows a linear ion trap configuration based on a cylinder that has been cut along its length into eight sectors, four at 60° angular width and four at 30° angular width. The quadrupole requirement, $\Phi(\rho,\theta \pm \pi/2) = -\Phi(\rho,\theta)$, leads to the expansion for the potential inside the cylindrical linear trap

$$\Phi(\rho,\theta) = C_0\rho^2\sin(2\theta) + C_1\rho^6\sin(6\theta) + C_2\rho^{10}\sin(10\theta) + \ldots$$

If the 30° sectors are grounded and the remaining 60° sectors are biased in a quadrupole fashion as shown, the resulting field is very harmonic, i.e., $C_1 = 0$.

An approximate implementation of this 60°/30° arrangement is shown in Figure 5. It consists of 12 circular rods with every 3rd rod grounded with the two intervening rods held at the same potential. This arrangement has the same 60°/30° symmetry of the sectored cylinder.

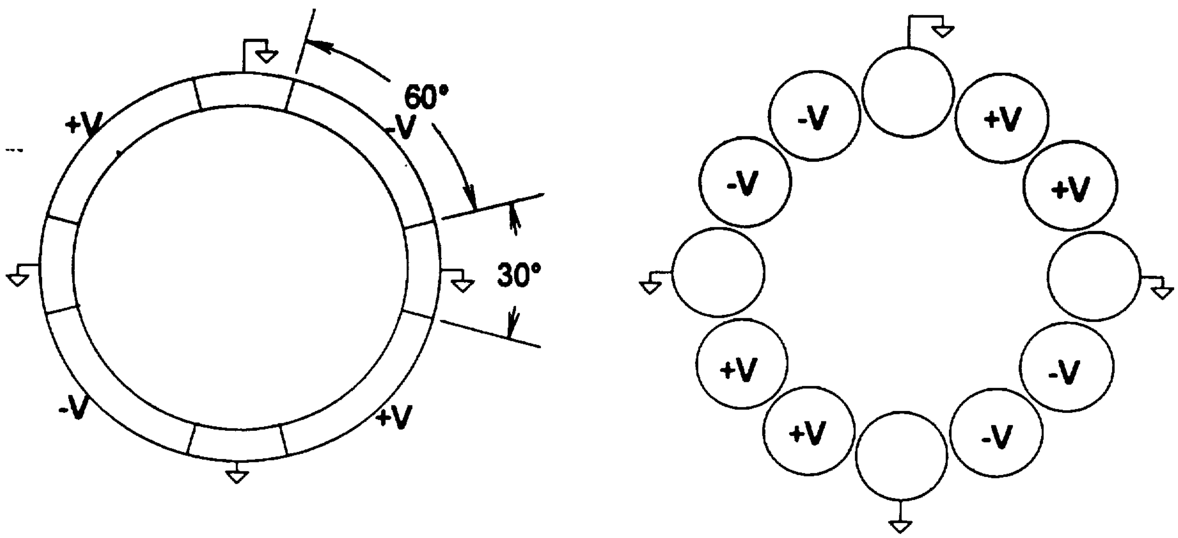

Figure 5. The trap on the left produces a very harmonic trap potential $\Phi(\rho,\theta) = C_0\rho^2\sin(2\theta) + C_2\rho^{10}\sin(10\theta) + \ldots$. The trap on the right is an approximate implementation of the 60°/30° symmetry constructed with 12 round rods.

ION CLOUD SIZE MEASUREMENT

The four auxiliary grounded rods can be used to generate a quadrupole magnetic field inside the linear trap whose node line coincides with the node line of the rf trapping fields. The shift of the clock transition with applied magnetic field is quadratic, $\nu = \nu_0 + \alpha\,\mathbf{H}^2$ where $\mathbf{H}$ is the total applied field and α is the sensitivity factor; $\alpha = 97$ Hz/Gauss^2 = 97 μHz/mG^2 for the $^{199}Hg^+$ clock transition. If the field is the sum of a static homogeneous field, $\mathbf{H}_0$, along the trap axis and the transverse quadrupole field, $\mathbf{h}_\perp(\mathbf{r})$, from the four auxiliary trap rods we find $\nu = \nu_0 + \alpha\,(\mathbf{H}_0 + \mathbf{h}_\perp(\mathbf{r}))^2 = \nu_0 + \alpha\mathbf{H}_0^2 + \alpha\mathbf{h}_\perp^2$. Since $\mathbf{h}_\perp(\mathbf{r}) = h'(\hat{x}y + \hat{y}x)$ and therefore, $\mathbf{h}_\perp^2 = (h')^2\rho^2$, the magnetic shift of the clock transition grows quadratically with distance from the node line. The clock frequency is the average of this spatially varying field over the ion cloud distribution, $n(\rho)$. Thus, $\langle\nu\rangle = \nu_0 + \alpha\mathbf{H}_0^2 + \alpha\langle\rho^2\rangle(h')^2$ where the brackets, $\langle\ \rangle$, indicate average over the ion cloud distribution. A measurement of the frequency change of the clock transition when the transverse field $\mathbf{h}_\perp(\mathbf{r})$ is applied can yield a measurement of the ion cloud radius. The quantities which determine $\langle\rho^2\rangle$ are ion number, ion temperature, and the trap rf level and its resulting secular frequency, ω_{sec}. For a fixed secular frequency and buffer gas pressure, ion number and temperature are not independent thus a measurement of $\langle\rho^2\rangle$ could be used to servo the electron emission to hold the ion number (and temperature) constant.

To estimate the size of the shifts suppose $\langle\rho^2\rangle = 1$ mm^2 and h' = 20 mG/mm. The shift when the quadrupole field of this strength is switched on is 97 μHz/mG^2 $\times$ 1 mm^2 $\times$ 400 mG^2/mm^2 $\approx$ 40 mHz which corresponds to a 1×10^{-12} shift of the clock transition. With a trap radius $R \approx 5$ mm the field gradient produced at the center is $h' \approx (\mu_0 I)/(\pi R^2) \approx 20$ mG/mm at a quadrupole excitation current of $I = 125$ mA. Even with $\langle\rho^2\rangle = 0.1\ mm^2$, a 400 mA current will produce a 10^{-12} clock shift. A clock with $10^{-13}/\sqrt{\tau}$ short term stability will measure this offset to about 1% in a few minutes of averaging time, τ.

T_2 Relaxation in $h_\perp$ field gradient

One problem that must be avoided with this technique is relaxation of the high Q clock transition in the field gradient of the quadrupole magnetic field, $\mathbf{h}_\perp(\mathbf{r})$. This method depends upon the clock transition shifting an amount proportional to $\langle\rho^2\rangle$ with little or no reduction in the signal size and line-Q. Ion motion in the applied field gradient can mix the two Zeeman states $F = 1$, $m_F = \pm 1$ with the upper clock state $F = 1$, $m_F = 0$ and cause a rapid relaxation of the coherence between the two clock levels $F = 1$, $m_F = 0$ and $F = 0$, $m_F = 0$. The frequency spacing to these Zeeman levels increases at $\cong 1.4$ kHz per mG of applied field $\mathbf{H}_0$, which is typically about 50mG.

The trajectory of an ion in the ρ, θ plane determines the spectrum of time variation of the quadrupole field, $\mathbf{h}_\perp(\mathbf{r})$. The coherence in the clock transition will relax rapidly as this spectrum overlaps with the Zeeman states at $\omega_0 = \pm\gamma H_0$, where $\gamma/2\pi \cong 1.4$ kHz/mG. Harmonic motion through the trap center leads to a magnetic field variation at the secular frequency of the trap, ω_{sec}. These are the 'free particle' limits. When space-charge repulsion is important (as for a large cloud), these frequencies move down. Thus, it would appear that to avoid relaxation via mixing with the Zeeman states we must run the static field $\mathbf{H}_0$ high enough so that $\gamma H_0 > \omega_{sec}$. As the static field is increased the clock transition grows more sensitive to field variations and the clock is potentially less stable.

Relaxation rates to the Zeeman states from the upper clock state can be estimated from nmr relaxation rates given in the Redfield theory [5,6]. The time dependent magnetic field seen by an ion moving in the field gradient of $\mathbf{h}_\perp(\mathbf{r})$ can have spectral overlap with the frequency splitting to the Zeeman states $\omega_0 = \pm\gamma H_0$ thereby transferring atoms into this state. In this estimate, the rate at which this occurs is assumed to be the same as the rate of coherence loss in the clock transition. The transfer of population occurs at a rate $T_1^{-1} \approx \gamma^2 (h')^2 (S_x(\omega_0) + S_y(\omega_0))/2$ where we have used $|\vec{\nabla} H_x|^2 = |\vec{\nabla} H_y|^2 = (h')^2$ in the notation of ref [5]. The spectrum of the time variation of the field gradient seen by the moving ion $S_x(\omega) = S_y(\omega) \sim (2k_BT/m\omega_{sec}^2)(t_c(t_c^{-2}+(\omega - \omega_{sec})^2))^{-1}$ is assumed to be a Lorentzian shape centered on the ion secular frequency, ω_{sec}, with width determined by the ion collision rate, t_c^{-1}, which changes the phase of the ion secular motion within the trap. The spectrum is derived from a harmonic oscillator which is randomly re-phased at an average time interval of t_c. These collisions could be with other atoms or ions, or could be with the trap end confinement fields where each turn-around at the end cap field will disrupt the secular frequency phase. The collisions must be of sufficient strength to randomize the phase of the harmonic secular motion. The mean square amplitude of the transverse motion is $2k_BT/m\omega_{sec}^2 = \langle\rho^2\rangle$, determined by the secular confinement and the ion temperature, T. We re-write the population rate transfer in terms of the frequency shift when the quadrupole field is applied, $\delta\nu = \alpha\langle\rho^2\rangle(h')^2$, as $T_1^{-1} \approx \gamma^2 (\delta\nu/\alpha)(t_c(t_c^{-2}+(\omega_0 - \omega_{sec})^2))^{-1}$. Taking $t_c \sim 1$ msec, $\omega_0-\omega_{sec} = 2\pi\ 50$ kHz, and $\delta\nu = 40$ mHz, we find that $T_1^{-1} \approx 300$/sec, a very rapid loss of coherence in the clock transition.

One possible solution to this near resonance relaxation is to apply the quadrupole field at a frequency, Ω, much higher than the secular frequency, ω_{sec}. Since along the path of the ion trajectory, $\mathbf{h}_\perp(\mathbf{r}(t)) = h'(\hat{x}y + \hat{y}x) = h_0'\cos\Omega t\,(y_0\sin\omega_{sec}t\ \hat{x} + x_0\sin(\omega_{sec}t + \phi)\,\hat{y})$, the frequencies of the quadrupole field seen by the moving ion are now up-shifted to $\Omega \pm \omega_{sec}$ which can be 10 or more times higher than γH_0 to avoid the mixing to the Zeeman states and loss of coherence in the clock transition. In this case the dominant frequency seen by the moving ion is $\sim\Omega$ so that $T_1^{-1} \approx \gamma^2 (\delta\nu/\alpha)(t_c(t_c^{-2}+(\omega_0 - \Omega)^2))^{-1}$. If the quadrupole field is applied at 2 MHz the relaxation rate is , $T_1^{-1} \approx 0.2$ /sec, much slower than with the dc quadrupole current and thereby preserving the line Q and signal size.

CLOCK COMPARISONS TO TEST FOR ALPHA VARIATION

A stringent test of modern grand unified theories can be carried out in laboratory clock frequency comparisons. Some theories [ref] predict a slow time variation of the fine structure constant, $\alpha = e^2/2\pi\hbar c$, due to the expansion of the universe. Because α describes the strength of electromagnetism, its time variation would lead to a slow time variation of all atomic energy level spacings. There have been several attempts to find a changing α by comparing clocks or spectral lines of different "electromagnetic composition" that is, atomic transitions which have a different dependence on α. Thus, a microwave superconducting cavity oscillator frequency was compared to a hydrogen maser transition frequency [7], fine structure intervals in Mg were compared to the hydrogen maser interval [8], and more recently, multiple spectral lines from quasars with large cosmological redshifts were compared [9]. In the quasar spectral data, there is evidence that during the early universe α differed from its present day value by $\Delta\alpha/\alpha = -2.64(\pm 0.35)\times 10^{-5}$. Although among the most precise measurements carried out, atomic clock rate comparisons were thought to be insensitive to any change in α since it was believed that all hyperfine clock transitions scaled with α in the same manner. We recently showed [10] that the relativistic hyperfine interaction strongly violates the uniformity of scaling with α as the atomic number Z of the clock atom increases. Thus a changing fine structure constant would force a fractional frequency change between the hydrogen hyperfine frequency, $\nu_{hydrogen}$, and an alkali atom or ion hyperfine frequency, ν_{Alkali}, according to [10]

$$\frac{\dot{\nu}_{Alkali}}{\nu_{Alkali}} - \frac{\dot{\nu}_{hydrogen}}{\nu_{hydrogen}} = (\alpha Z)^2 \frac{12\lambda^2 - 1}{\lambda^2(4\lambda^2 - 1)} \frac{1}{\alpha}\frac{d\alpha}{dt} \equiv L_d F_{rel}(\alpha Z)\frac{1}{\alpha}\frac{d\alpha}{dt}$$

where $\lambda = [1-(\alpha Z)^2]^{1/2}$. We compared a LITS Hg^+ clock frequency to a hydrogen maser frequency for 140 days to limit fractional changes in α to be less than $\sim 4\times 10^{-14}$/year. Comparing laser cooled atomic clocks, for example, Rb vs Cs, could measure any linear variation in α larger than $\sim 10^{-16}$/year [11], as good as the best limits placed on a time variation of α [12].

A much more stringent search for an α variation can be carried out by searching for a spatial dependence of α in the strong gravitational potential at four solar radii, where gravitational time dilation slows all clocks by $\sim$1 micro-second per second as compared to Earth-based clocks. Because an expanding universe presumably drives a time variation in α, we write

$$\frac{d\alpha}{dt} = \frac{d\alpha}{dU/c^2}\frac{dU/c^2}{dt} = \frac{d\alpha}{dU/c^2}H$$

Where H $\sim 10^{-10}$/year is the Hubble constant. Thus two or more clocks as payload on a four solar radii solar flyby, whose relative rates are compared, could probe for a dependence of α on U_{solar}. Since time dilation effects are $\sim 10^{-6}$ at four solar radii, clocks based on atoms of sufficiently different atomic number Z, with differential stability $\sim 10^{-16}$ could probe for $d\alpha/dU$ at the 10^{-10} level. This would reveal any time variation in α larger than 10^{-20} per year. The design of a spacecraft that can survive and function on a four solar radii flyby, where the solar flux is 4 Mega-Watts per meter^2, has been studied at JPL for many years.

ACKNOWLEDGMENTS

This work was carried out at the Jet Propulsion Laboratory, California Institute of Technology, under a contract with the National Aeronautics and Space Administration.

REFERENCES

1. J. D. Prestage, G. J. Dick, and L. Maleki, *J. Appl. Phys.* **66**, 1013-1017 (1989).
2. R. J. Tjoelker, J. D. Prestage, and L. Maleki, "A Mercury Linear Ion Trap Frequency Standard for the USNO," in *Proceedings of the 1995 IEEE International Frequency Control Symposium*, 1995, pp. 79-81.
3. J. D. Prestage, R. L. Tjoelker, G. J. Dick, and L. Maleki, "Improved Linear Ion Trap Physics Package," *Proceedings of the 1993 IEEE International Frequency Control Symposium*, 1993, pp. 144-147.
4. G. John Dick, Rabi T. Wang, and Robert L. Tjoelker, "Cryo-Cooled Sapphire Oscillator with Ultra-High Stability," *Proceedings of the 1998 IEEE International Frequency Control Symposium*, 1998, pp. 528-533.
5. D. D. McGregor, *Phys. Rev. A* 41, 2631 (1990).

6. C. P. Slichter, *Principles of Magnetic Resonance* (Harper and Row, New York, 1963), Sec. 5.7.
7. J. P. Turneaure and S. Stein, *Atomic Masses and Fundamental Constants V* (Plenum, London, 1976), pp. 636-642.
8. A. Godone, C. Novero, P. Tavella and K. Rahimullah, *Phys. Rev. Lett.* 71, pp. 2364-2366 (1993).
9. J. K. Webb et. al., to appear in *Phys. Rev. Lett.*
10. J. D. Prestage, R. L. Tjoelker, and L. Maleki, *Phys. Rev. Lett.* 74, 3511-3514 (1995).
11. Private Communication, Ch. Salomon and A. Clairon.
12. Th. Damour and F Dyson, *Nuc. Phys. B* 480, 37-60 (1996).